Article

Current Biology

Sleep Spindle Refractoriness Segregates Periods of Memory Reactivation

Highlights

- Reactivating memories with auditory cues during sleep benefited retention
- Sleep spindle power increased after cues and predicted subsequent memory
- Cue efficacy was impaired when cues fell within the spindle refractory period
- The importance of spindle timing was confirmed using real-time spindle tracking

Authors

James W. Antony, Luis Piloto, Margaret Wang, Paula Pacheco, Kenneth A. Norman, Ken A. Paller

Correspondence

jantony@princeton.edu

In Brief

Current memory models posit that declarative memory retention benefits from brief bursts of activity called sleep spindles. Using auditory cues to target memories during sleep and a real-time algorithm to track sleep spindles in the EEG, Antony et al. show that optimal memory reactivation is linked to rhythmic changes in spindle likelihood.

Antony et al., 2018, Current Biology *28*, 1–8
June 4, 2018
https://doi.org/10.1016/j.cub.2018.04.020

CellPress

Please cite this article in press as: Antony et al., Sleep Spindle Refractoriness Segregates Periods of Memory Reactivation, Current Biology (2018), https://doi.org/10.1016/j.cub.2018.04.020

Current Biology
Article

Sleep Spindle Refractoriness Segregates Periods of Memory Reactivation

James W. Antony,[1,3,*] Luis Piloto,[1] Margaret Wang,[1] Paula Pacheco,[1] Kenneth A. Norman,[1] and Ken A. Paller[2]
[1]Princeton Neuroscience Institute, Princeton University, Princeton, NJ 08544, USA
[2]Department of Psychology, Northwestern University, Evanston, IL 60208, USA
[3]Lead Contact
*Correspondence: jantony@princeton.edu
https://doi.org/10.1016/j.cub.2018.04.020

SUMMARY

The stability of long-term memories is enhanced by reactivation during sleep. Correlative evidence has linked memory reactivation with thalamocortical sleep spindles, although their functional role is not fully understood. Our initial study replicated this correlation and also demonstrated a novel rhythmicity to spindles, such that a spindle is more likely to occur approximately 3–6 s following a prior spindle. We leveraged this rhythmicity to test the role of spindles in memory by using real-time spindle tracking to present cues within versus just after the presumptive refractory period; as predicted, cues presented just after the refractory period led to better memory. Our findings demonstrate a precise temporal link between sleep spindles and memory reactivation. Moreover, they reveal a previously undescribed neural mechanism whereby spindles may segment sleep into two distinct substates: prime opportunities for reactivation and gaps that segregate reactivation events.

INTRODUCTION

Memories of daytime episodes are covertly reactivated during sleep, improving memory storage in the brain [1]. Previous research has implicated three electrophysiological signals in declarative memory processing during sleep. The slowest of these are slow oscillations (SOs), brain rhythms at approximately 1 Hz prominent during deep sleep [2] that improve memory when externally enhanced [3, 4]. A second signal is the sleep spindle, a burst of thalamocortical activity at 11–16 Hz lasting 0.5–3 s. Third, replay of newly formed memories is thought to occur in conjunction with high-frequency bursts of hippocampal and cortical activity called ripples [1, 5, 6]. These three signals can occur with precise temporal relationships; spindles tend to occur most often during the up-state phase of SOs, and ripples tend to occur at spindle troughs [7–9]. To the extent that these temporal relationships are evident, memory consolidation appears to be more effective [10], suggesting a dual cross-frequency coupling mechanism by which hippocampal-dependent memories become stabilized in long-term neocortical networks over time [2].

Previous studies have linked spindles and memory on multiple timescales. On a long timescale, memory measures positively correlate with spindle measures accumulated over full sleep periods [11–21]. On a short timescale, studies using targeted memory reactivation (TMR [22], a technique where learning-related auditory cues are presented during sleep to promote replay) have found that individual spindles increase shortly after the presentation of auditory cues that boost memory [23–26]. However, how reactivation unfolds over time in relation to successive spindles is largely unknown. Prior *in vitro* [27, 28], *in vivo* [29], and human EEG [30] evidence indicates that spindles are unlikely to occur shortly after other spindles, indicative of a refractory period. If spindles play a crucial role in memory reactivation, then reactivation and associated benefits for subsequent memory should be less likely during the refractory period.

Here, we investigated and manipulated temporal relationships between spindles and TMR cues. In all experiments (Figure 1A), subjects first over-learned novel associations between individual sounds and picture items (e.g., [meow]-Brad Pitt, [violin]-Eiffel Tower). Next, they learned unique locations for each item on a background grid. After an initial test, they took an afternoon nap with background white noise (~40 dB; Table S1 provides sleep-stage information). Upon online indications of slow-wave sleep (SWS), we embedded cues in the noise, one every 4.5 s. After a post-nap break, subjects took tests on both item-location associations and sound-item associations. In the first two experiments, we found post-cue spindle power positively predicted memory retention, whereas pre-cue spindle power negatively predicted retention. We suspected the latter effect occurred because cues fell within the spindle refractory period. We designed experiment 3 to test this idea directly by tracking spindles in real time and presenting cues at different times relative to spindle onsets; in this experiment, we found strong evidence that cues presented immediately after the refractory period led to superior memory.

RESULTS

Retention Was Enhanced by Cues and Predicted by Post-cue Spindles

In all experiments, we analyzed spatial forgetting by subtracting pre-nap error from post-nap error and regressing out pre-nap error to produce a memory change score (Figure S1). In experiment 1 (N = 18), we presented only half of the cues during sleep and contrasted memory retention for cued versus uncued items.

Please cite this article in press as: Antony et al., Sleep Spindle Refractoriness Segregates Periods of Memory Reactivation, Current Biology (2018), https://doi.org/10.1016/j.cub.2018.04.020

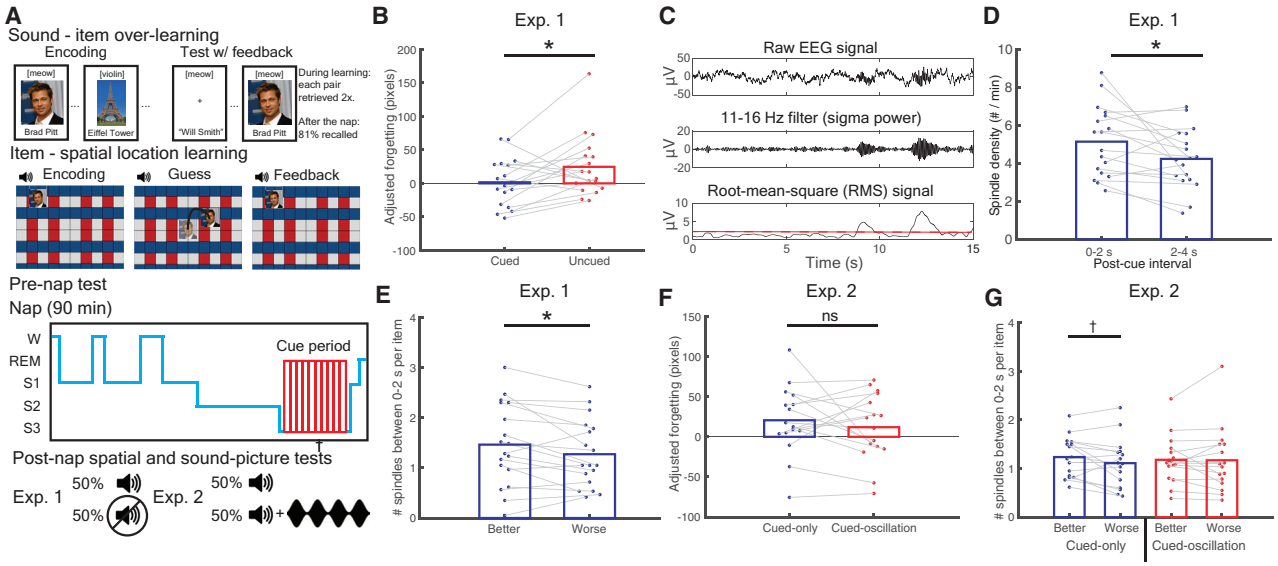

Figure 1. Experiments 1 and 2: Procedure and Post-cue Spindle Results

(A) Subjects over-learned associations between sounds and items before learning item spatial locations. In experiment 1, half of the sounds were presented during slow-wave sleep (SWS) of an afternoon nap. In experiment 2, all sounds were similarly presented, and half were followed by 15 Hz, oscillating white noise (cued-oscillation).

(B) In experiment 1, cues reduced forgetting between pre-nap and post-nap tests.

(C) Sleep spindle calculation.

(D) During the 2 s immediately after cues (0–2 s) relative to the next 2 s (2–4 s), centroparietal spindles were increased.

(E) A median split analysis showed more early spindles per item predicted better memory.

(F) In experiment 2, forgetting did not differ between cued-only and cued-oscillation conditions.

(G) Early spindles marginally indexed better memory for the cued-only condition but not the cued-oscillation condition.

$^{\dagger}p \leq 0.1$, $^{*}p \leq 0.05$; ns, not significant; REM, rapid eye movement; S1–S3, sleep stages 1–3; W, waking. All error measurements indicate SEM.

See also Figure S1 and Table S1.

As predicted [31–33], cues improved memory (in pixels, cued: 1.6 ± 8.4; uncued: 24.7 ± 10.9; $t(17) = 2.2$, $d_z = 0.5$, p = 0.039; within-subject correlation (r_{within}) = 0.44; Figure 1B).

We next investigated relationships between post-cue spindles and memory. We detected spindles by band passing sigma (11–16 Hz), calculating root-mean-square (RMS) values using sliding 200-ms intervals, and extracting above-threshold segments (STAR Methods; Figure 1C). We found that cues tended to provoke spindles, in line with previous findings [34, 35]. Spindles over a centroparietal cluster of five electrodes (Cz, CP3, CPz, CP4, Pz) increased early relative to later after cues (0–2 s versus 2–4 s, respectively; $t(17) = 2.3$, $d_z = 0.54$, p = 0.03, r_{within} = 0.53; Figure 1D). Furthermore, a median-split analysis (dividing above versus below each subject's median forgetting value) revealed that more spindles occurred within 2 s after better-remembered items than after worse-remembered items ($t(17)$ = 2.23, $d_z = 0.53$, p = 0.039, $r_{within} = 0.9$; Figure 1E). Therefore, as in several prior studies [23–26], post-cue spindle activity positively predicted memory.

Post-cue Oscillating Auditory Rhythms Had No Effect on Post-cue Spindles or Memory

We next sought to move beyond the above correlative evidence by manipulating the incidence of post-cue spindles and determining whether conditions that boost spindle occurrence also boost subsequent memory. First, we attempted to boost spindles directly using sensory-entrainment methods. Subjects in experiment 2 (N = 16) followed a similar cueing paradigm during sleep, except half of the cues were presented alone (cued-only) and half were followed by 2 s of white noise amplitude modulated at a spindle frequency (15 Hz; cued-oscillation). Given that such white-noise oscillations were previously found to facilitate spindles [35], we hypothesized that cued-oscillation sounds would show greater post-cue spindles as well as better retention for those cued items. Contrary to our expectations, cues with oscillating sounds versus cues presented alone were not associated with differences in incidence of 0–2 s post-cue spindles ($t(15)$ = 0.20, $d_z = 0.05$, p = 0.84, $r_{within} = 0.86$) or in corresponding memory performance (in pixels, cued-only: 20.6 ± 10.7; cued-oscillation: 12.0 ± 10.4; $t(15) = 0.8$, $d_z = 0.2$, p = 0.44, $r_{within} = 0.47$; Figure 1F). Unlike in our prior study [35], oscillating sounds did not increase spindle incidence. We further probed for memory effects by submitting spindle density to a cue condition (cued-only versus cued-oscillation) x median-split subsequent memory (better versus worse) repeated-measures ANOVA. We found no significant main effect of subsequent memory ($F(1,15) = 2.4$, p = 0.14) or cue condition ($F(1,15) = 0.001$, p = 0.97) or interaction ($F(1,15) = 1.0$, p = 0.33). We then considered whether oscillatory stimulation could have disrupted the relationship between spindles and memory. Given the spindle-memory relationships found in experiment 1, we tested the two stimulation conditions separately. We found a marginal trend for more spindles for better

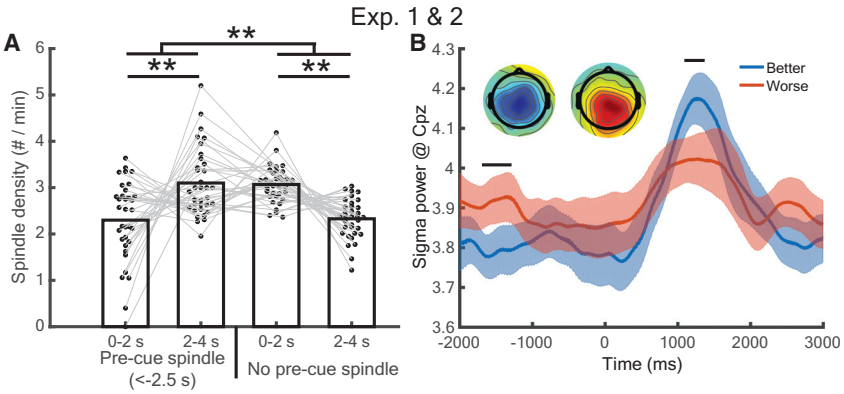

Figure 2. Pre-cue Spindles Prevented Post-cue Spindle Increases and Negatively Predicted Memory Retention

(A) Analyses across both experiments revealed that pre-cue spindles (occurring −2.5 to 0 s) reversed the prevalence of early versus late post-cue spindles. **p < 0.01.

(B) Better-remembered items showed higher post-cue but lower pre-cue sigma power than worse-remembered items. Horizontal bars indicate significant time segments (p < 0.05). Inset: topographical maps of RMS values for better versus worse memory centered around −1,550 and 1,300 ms, respectively. All error measurements indicate SEM.

than worse memory in the cued-only condition ($t(15) = 1.78$, $d_z = 0.44$, p = 0.096, $r_{within} = 0.83$) but not the cued-oscillation condition ($t(15) = 0.13$, $d_z = 0.03$, p = 0.90, $r_{within} = 0.91$; Figure 1G).

Pre-cue Spindles Prevented Post-cue Spindle Boosts, and Pre-cue Sigma (Spindle Band) Power Negatively Predicted Memory

Given that the cued-oscillation approach did not work as expected, we next explored whether spindles were modulated by the time since the prior spindle occurrence, in keeping with the evidence outlined above for spindle refractory periods. As an initial probe into this question, we asked whether the presence of a pre-cue spindle influenced post-cue spindle probability. Combining data from experiment 1 and both cueing groups of experiment 2, we found a significant interaction between whether there was a pre-cue spindle (−2.5 to 0 s) and early-versus-late post-cue spindle rate (0–2 s versus 2–4 s, respectively; $F(1,33) = 24.23$, p < 0.001). When pre-cue spindles were present, there were more late than early post-cue spindles ($t(33) = 3.1$, $d_z = 0.53$, p = 0.004, $r_{within} = -0.78$); when pre-cue spindles were absent, there were more early than late post-cue spindles ($t(33) = 5.5$, $d_z = 0.94$, p < 0.001, $r_{within} = -0.86$) (Figure 2A). Thus, cues may generally promote spindles within 2 s of cue onset, but this spindle boost is less likely for a cue that was immediately preceded by a spindle.

We then asked whether pre-cue spindle activity negatively affected memory by analyzing cue-locked sigma power at electrode CPz while correcting for multiple comparisons. As expected, sigma power was higher for better- than worse-remembered items for a post-cue time segment (1,092 to 1,372 ms; p < 0.05) but higher for worse- than better-remembered items during a pre-cue time segment (−1,696 to −1,288 ms; p < 0.05) (Figure 2B). We additionally submitted RMS sigma power for these segments to a time period (pre-cue versus post-cue) x median-split memory (better versus worse) repeated-measures ANOVA. We found a significant main effect of time ($F(1,33) = 9.2$, p = 0.005) and interaction between time and memory ($F(1,33) = 9.7$, p = 0.004) but no main effect of memory ($F(1,33) = 0.58$, p = 0.45). These results hinted that memories cued within spindle refractory periods may be unlikely to undergo reactivation. However, whereas we found a subsequent memory difference for pre-cue sigma power, we did not find a direct subsequent memory effect for pre-cue spindles from −2.5 to 0, as quantized by our algorithm (better: 0.156 ± 0.013; worse: 0.16 ± 0.017; $t(33) = 0.43$, $d_z = 0.07$, p = 0.67, $r_{within} = 0.8$).

Sigma (Spindle Band) Power Exhibits a 0.17–0.33 Hz Rhythmicity

To further understand these spindle refractory effects, we computed the inter-spindle lag (Figure 3A). Inter-spindle lag analyses showed there were fewer spindles at lags of 1–2.5 s (13.4% ± 0.8%) compared to 2.5–4 s (23.3% ± 0.9%; $t(33) = 8.1$, $d_z = 1.4$, p < 0.001, $r_{within} = 0.03$). A parallel analysis in the frequency domain revealed a peak at 0.21 Hz (4.8 s inter-spindle lag) with a range around the peak at 0.17–0.33 Hz (3–5.9 s inter-spindle lag; Figure 3B). These results revealed that sigma activity, itself indexing oscillatory activity (at 11–16 Hz), occurs not randomly but with a slower oscillatory rhythm (at 0.17–0.33 Hz). Additionally, we found a strong peak at an infra-slow frequency (~0.02 Hz), in line with a recent report suggesting the presence of spindle-rich intervals separated by ~50 s [36].

The above analyses demonstrated frequency peaks in sigma activity when measured over the full sleep period. Next, we zoomed in on the activity surrounding spindles themselves. We obtained sigma RMS values of −10 to 10 s around the RMS peaks of verified spindles (Figure 3C) and then performed autocorrelations between each time lag and the RMS peak for each subject. The autocorrelation graph revealed "reverberations" of positive and negative peaks in sigma power, most likely corresponding to spindles and refractory periods between spindles. On each side of $t = 0$, there were negative, positive, negative, and positive peaks (approximately ±1.5, ±3.1, ±4.6, and ±5.7 s, respectively; Figure 3D; Table S2). These analyses depict the overall rhythmicity presented above on a shorter timescale. To ensure these qualitative results were not artifacts of cueing, we analyzed data from subjects who did not receive cues from different experiments (N = 28; STAR Methods; Figure S2). All major aspects of the above analyses held, except reverberation cycles were slightly wider (~4 s rather than ~3 s).

Finally, as both preceding spindles and sounds affect spindle occurrence, we measured the interaction of these two variables to assess their relative impact (Figure 3E). We measured the bivariate likelihood of a spindle occurring within 0.5 s time bins from 0–4.5 s after cues and 0–10 s after preceding spindles. In line with previous analyses, spindles were most likely 3–6 s after predecessors and shortly after cues. Interestingly, sounds

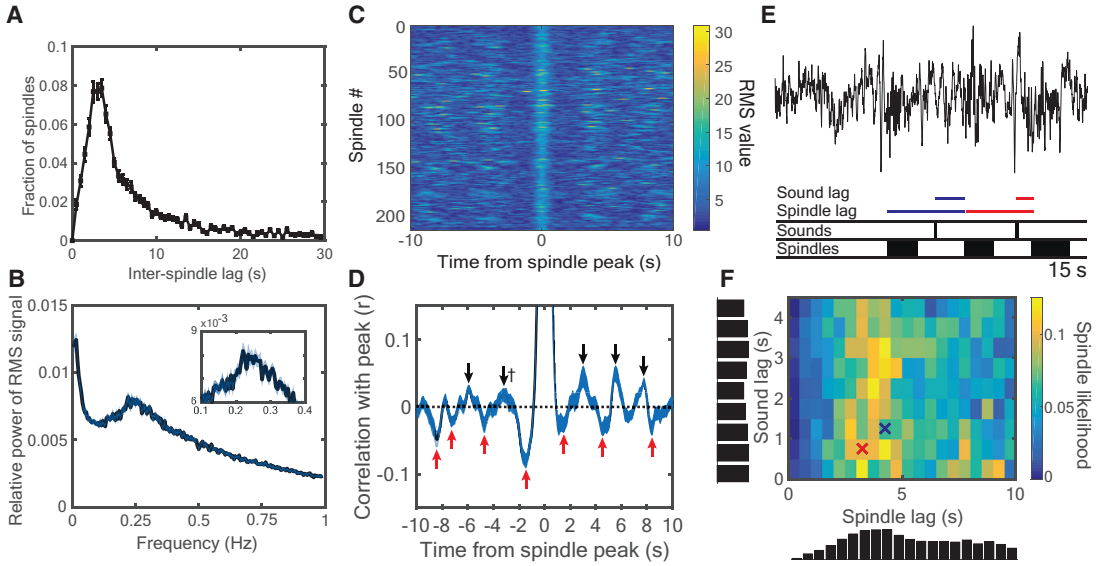

Figure 3. Characterizing the Spindle Refractory Period

(A) Inter-spindle lags (ISLs) were calculated as the time between the start of successive spindles, shown for up to 30 s.

(B) Fast Fourier transformations of the sigma RMS signal revealed cyclic activity most prominent in the 0.17–0.33 Hz range, corresponding to ISLs in the range of 3–5.9 s.

(C) RMS values spanning from −10 to +10 s surrounding spindle peaks from one sample subject.

(D) Correlations between the RMS value of the spindle peak and all other values from −10 to 10 s were calculated for each subject. The correlation was $r = 1.0$ at the $t = 0$ spindle peak. All positive (black) and negative (red) peaks that significantly differed from zero across subjects ($p < 0.05$) are marked with arrows, except the dagger indicates $p = 0.07$. See also Table S2.

(E) For each instant along the recording, we queried whether a spindle started or not and the time lags since the last spindle and last sound cue.

(F) Likelihoods of spindles starting as a joint function of spindle and sound lag. Vertical and horizontal histograms indicate cumulative spindle likelihood within each row and column, respectively. Crosses indicate bins corresponding to color-coded time lags from (E).

All error measurements indicate SEM. See also Figure S2.

shortly after spindles resulted in few spindles, whereas spindles frequently occurred 3–6 s after preceding spindles almost regardless of cues (Figure 3F). To quantify this, we contrasted the across-subject mean spindle likelihood between two different two-dimensional bins. The first refers to a period shortly after cues and shortly after spindles, during which the early post-cue spindle boost might have been prevented by a preceding spindle (0–2 s post-cue and 1–2.5 s post-spindle). The second refers to a period during which cues should have very little influence on spindles but is a more optimal time lag given spindle rhythmicity (2–4 s post-cue and 2.5–4 s post-spindle). We found significantly more spindles in the latter two-dimensional bin (7.5% ± 0.6% versus 2.5% ± 0.5%; $t(19) = 5.6$, $d_z = 0.97$, $p < 0.001$, $r_{within} = -0.19$). These results suggest the spindle refractory period imposes a limitation on spindle probability that mostly overrides sensory influences.

Cues Presented Outside of the Spindle Refractory Period Led to Better Memory

Given these results, we therefore reasoned that it should be possible to control spindle probability by manipulating the timing of the cue relative to the last spindle: cues presented in the spindle refractory period should be less likely to trigger spindles and should lead to worse memory relative to cues presented outside of the refractory period. To test this hypothesis, in experiment 3 (N = 20), we developed an algorithm to track spindles in real time (Figure 4A), and we used this algorithm to deliver cues at systematically different times relative to preceding spindles. Each cue was presented either shortly after a spindle finished (0.25 s, early condition) or much later (~2.5 s, late condition). As a manipulation check, offline analysis showed a far greater incidence of pre-cue spindles (from −2.5 s to 0 s relative to cue onset) for early cues compared to late cues (early: 40.4% ± 2.4%; late: 5.7% ± 1.1%; $t(19) = 13.3$, $d_z = 2.97$, $p < 0.001$, $r_{within} = 0.05$; Figure 4B). Crucially, spatial memory was more accurate with late cues compared to early cues (in pixels, early: 29.7 ± 10.4; late: 2.7 ± 8.5; $t(19) = 3.2$, $d_z = 0.7$, $p = 0.004$, $r_{within} = 0.62$; Figure 4C). That is, memory reactivation was apparently reduced within the spindle refractory period, suggesting that when spindles are unlikely, reactivation is unlikely.

To verify the predominance of spindles shortly after late cues, we submitted spindle-density measures to a cue type (early versus late) x post-cue interval (0–2 versus 2–4 s) ANOVA. We found a significant interaction between cue type and post-cue interval ($F(1,19) = 6.6$, $p = 0.01$; Figure 4D). Spindles increased 0–2 s (versus 2–4 s) after late cues ($t(19) = 4.0$, $d_z = 0.88$, $p < 0.001$, $r_{within} = 0.19$) but not after early cues ($t(19) = 0.44$, $d_z = 0.10$, $p = 0.66$, $r_{within} = 0.09$). Because stimulus-evoked SOs predict memory retention [3] and have also been shown to have refractory periods [37, 38], we next wanted to verify that effects that are attributed here to the spindle refractory period were not due instead to the SO refractory period. The same

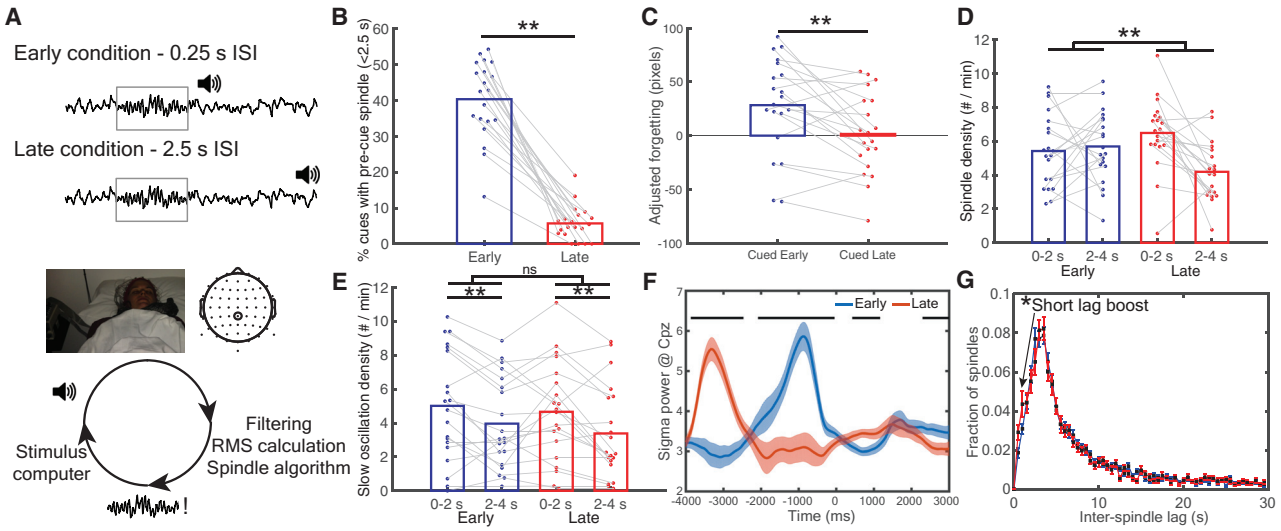

Figure 4. Memory Retention Was Impaired for Items Cued Inside versus Outside the Spindle Refractory Period

(A) Top: in experiment 3, TMR cues were presented either early or late after a spindle was detected, placing them (respectively) inside or outside the spindle refractory period. Bottom: real-time schematic. EEG traces from electrode CPz were filtered between 11 and 16 Hz, the RMS signal was calculated, and detected spindles were sent to another computer to present cues at the appropriate times. See also Figure S3.

(B) A manipulation check showed a higher percentage of pre-cue spindles (<2.5 s) in the early than late cued conditions.

(C) Late cues significantly enhanced memory retention relative to early cues.

(D) Late cues showed a significant spindle boost early in the post-cue interval, whereas early cues did not.

(E) Both early and late cues boosted SOs, but there was no interaction between conditions.

(F) Cue-locked analyses revealed higher early post-cue sigma power for late relative to early cues. All horizontal bars indicate $p < 0.05$ segments.

(G) Comparison of inter-spindle lags in experiments 1 and 2 versus experiment 3 revealed an increased number of very short inter-spindle lags.

**$p < 0.01$. All error measurements indicate SEM.

See also Table S1.

analyses on SOs, as measured using established algorithms [4], revealed more SOs 0–2 versus 2–4 s after cues (0–2 s: 4.84 ± 0.67; 2–4 s: 3.67 ± 0.58; $F(1,19) = 11.66$, $p < 0.001$) but no effect of our early-versus-late cueing manipulation (early: 4.48 ± 0.64; late: 4.02 ± 0.61; $F(1,19) = 2.8$, $p = 0.11$) or interaction ($F(1,19) = 0.6$, $p = 0.44$) (Figure 4E), indicating that the observed memory effects of this manipulation are unlikely to be due to modulation of SOs. To show the specificity of this interaction to spindles (as opposed to SOs), we submitted event-density measures to a cue type (early versus late) x post-cue interval (0–2 versus 2–4 s) x event type (spindles versus SOs) repeated-measures ANOVA, which produced a significant three-way interaction ($F(1,19) = 5.05$, $p < 0.037$).

The reverberatory nature of sigma power was also evident in temporal patterns of cue-locked sigma RMS differences between early and late cues (Figure 4F): late cues, higher from −3,868 to −2,472 ms; early, higher from −1,992 to −48 ms; late, crucially higher from 500 to 1,172 ms; early, higher from 2,252 to 3,000 ms (all segments corrected for multiple comparisons). To ask whether higher sigma power for late cues was related to memory, we divided late cues into better- versus worse-remembered associations using a median split. We found one brief segment of significant time points (420–564 ms, significant at the $p < 0.05$ level) showing higher sigma power for better- than worse-remembered associations. However, this segment did not survive cluster correction in a permutation test for multiple comparisons ($p = 0.07$). Finally, because *in vivo* evidence suggests the refractory period is not absolute [29, 39], we reasoned that early cues directly after spindles should still occasionally elicit spindles. This should emerge as an increase in spindles at very short ISLs relative to experiments 1 and 2 (which did not systematically present cues immediately following previous spindles). In keeping with this idea, we found higher proportions of spindles at very short lags (<1.5 s) in experiment 3 than experiments 1 and 2 combined (experiments 1 and 2: 4.9% ± 0.5%; experiment 3: 7.3% ± 1.0%; $t(52) = 2.38$, $d = 0.67$, $p = 0.02$; Figure 4G).

Over-Learned Sound-Item Associations Were Well Remembered Post-nap

We additionally tested over-learned sound-item memory (e.g., [meow]-Brad Pitt) after the final spatial item-location test to assess whether these associations were still well remembered post-nap. Although we expected ceiling-level performance, it is conceivable that cueing could also strengthen these associations. Overall, these results showed non-significant TMR benefits that were weaker than, but generally consistent with, the spatial error results in each experiment. In experiment 1, cued associations were marginally better remembered than uncued associations (cued: 0.82 ± 0.04; uncued: 0.80 ± 0.05; $t(17) = 1.7$, $d_z = 0.4$, $p = 0.106$, $r_{within} = 0.96$). In experiment 2, no difference was found between cued-only and cued-oscillation associations (cued-only: 0.77 ± 0.04; cued-oscillation: 0.80 ± 0.03; $t(15) = 0.93$, $d_z = 0.23$, $p = 0.37$, $r_{within} = 0.67$). In experiment 3, late cued associations were marginally better remembered than early cued associations (early: 0.745 ± 0.03; late: 0.794 ± 0.02; $t(19) = 1.8$, $d_z = 0.4$, $p = 0.089$, $r_{within} = 0.46$).

DISCUSSION

Here we present converging evidence showing a previously under-characterized rhythm of spindle incidence, corresponding to a 3–6 s inter-spindle lag that is strongly linked to memory reactivation. At inter-spindle lags of <3 s (left side of Figure 3F), the state of local thalamocortical spindle networks is presumably refractory due to the hyperpolarization-activated current, I_h [27, 28]. At inter-spindle lags of >6 s (right side of Figure 3F), the reduced spindle likelihood may reflect the initial shift to a subtly different physiological state less conducive to spindles, even with the presentation of cues. Additionally, we replicated a recently discovered sigma activity peak at an infraslow frequency (~0.02 Hz; Figure 3B) [36]. Our findings underscore the importance of considering spindles on the meso-scale (~0.2–0.3 Hz), intermediate between the sub-second scale of the oscillations themselves (11–16 Hz) and the infraslow scale just under a minute (0.02 Hz).

In these experiments, we linked spindle potentiality over centroparietal EEG sources with declarative memory reactivation. However, previous studies using thalamocortical field potentials [29], magnetocephalography [40], and electrocorticography [41, 42] suggest a complex story whereby spindles occur on multiple spatial scales from local to global, of which EEG spindles largely detect the latter. Interestingly, refractory periods appear to occur locally, as recent local spindles affect their likelihood of participating in newly emerging global spindles [29]. We anticipate future research that can elucidate whether memory processing is differentially affected by local versus global spindles or local spindles from different sources.

These findings parallel and qualify recent investigations into memory reactivation with respect to SOs. Given that SOs nest spindles and ripples [9], they could be seen to segment and thereby regulate memory reactivation. In humans, boosting SOs improves memory [3, 43]; however, the degree to which it improves memory may be limited to effects on spindles [4, 37]. Here we provide additional evidence that reactivation may be more broadly regulated by the spindle refractory period (~3–6 s) than individual SOs (~1 s). We speculate that this regulation could serve as a mechanism for segregating memory reactivation related to different events.

Additionally, whereas stimulation to enhance SOs [4, 37] and the presentation of TMR cues [44, 45] are most effective at particular SO phases, our findings show that TMR is most effective at particular "phases" of the meso-scale sigma power rhythm of 0.2–0.3 Hz. Efforts to manipulate spindles via optogenetic [46] or auditory [35] stimulation may likewise benefit by considering this rhythm.

Another proposed function of spindles is in the gating of sensory processing during sleep [47, 48]. This idea stems from prior data showing that spindles increase due to sensory stimulation [34, 35, 49] and, in turn, neural responses to stimuli decrease during spindles [49–51]. There are three aspects of the current findings that are relevant to this idea. First, in accord with the finding that stimuli increase spindles, here we found that auditory stimulation elicited spindles (Figure 1D). Second, in designing experiment 3, we wanted to avoid the scenario in which early cues might simply undergo less processing because they were presented during ongoing spindles. Therefore, instead of concurrent stimulation, we presented early cues 250 ms after the spindle-detection algorithm indicated a spindle was completed. Indeed, we found no differences in sigma power between cueing conditions when cues began (Figure 4F). Third, a novel, related idea is that sensory signals themselves could be reduced during the spindle refractory period. If this were true, we should expect to see more evoked SOs for late than early cues in experiment 3, which could serve as a proxy for sensory processing [49, 51], during the interval shortly after cues. However, we found no such difference (Figure 4E). Nevertheless, we cannot rule out the possibility that early and late cues differed at some level of sensory processing. Moreover, further research is needed to determine whether these results apply to targeted more so than to spontaneous memory reactivation.

In conclusion, our findings suggest that optimal memory reactivation relies on spindle potentiality. Spindles apparently segment sleep into prime opportunities for reactivation interspersed by gaps corresponding to the spindle refractory period. These gaps may not constitute an obstacle for consolidation. Rather, we speculate that pauses between spindles may be beneficial for segregating reactivation events from each other. Spindle results obtained with and without the presentation of subtle memory cues furthermore suggest fundamental limitations on the amount and timing of reactivation that occurs across a given sleep period.

STAR★METHODS

Detailed methods are provided in the online version of this paper and include the following:

- KEY RESOURCES TABLE
- CONTACT FOR REAGENT AND RESOURCE SHARING
- EXPERIMENTAL MODEL AND SUBJECT DETAILS
  - Subjects
- METHOD DETAILS
  - Stimuli
  - Design
  - Procedure
  - EEG recording and pre-processing
  - Sleep physiological analyses
  - Real-time spindle algorithm
  - Spontaneous (non-TMR) sleep data
- QUANTIFICATION AND STATISTICAL ANALYSIS
  - Behavioral dependent variables and analyses
  - Physiological analyses
  - Spindle refractory period analyses
  - Experiment 3 physiological analyses
  - Sound-item memory analyses
- DATA AND SOFTWARE AVAILABILITY

SUPPLEMENTAL INFORMATION

Supplemental Information includes three figures and two tables and can be found with this article online at https://doi.org/10.1016/j.cub.2018.04.020.

ACKNOWLEDGMENTS

This work was supported by NIH grant F31-MH100958 and a CV Starr fellowship (to J.W.A.), and NSF grant BCS-1461088 (to K.A.P. and K.A.N.). We thank Neggin Keshavarzian for additional help collecting data, and Nick Depinto for

help with the real-time EEG setup. Pre-registered methods for experiment 3 along with data from all experiments at the time of publication can be found at https://osf.io/brndg/.

AUTHOR CONTRIBUTIONS

J.W.A., L.P., K.A.N., and K.A.P. conceived experiment 1. J.W.A. conceived experiments 2 and 3. M.W. contributed heavily to the real-time EEG code. J.W.A., M.W., and P.P. collected the data. J.W.A., L.P., K.A.N., and K.A.P. analyzed the data. J.W.A., K.A.N., and K.A.P. wrote the manuscript. All authors discussed the results and revised the paper.

DECLARATION OF INTERESTS

The authors declare no competing interests.

Received: February 5, 2018
Revised: March 14, 2018
Accepted: April 5, 2018
Published: May 24, 2018

REFERENCES

1. Wilson, M.A., and McNaughton, B.L. (1994). Reactivation of hippocampal ensemble memories during sleep. Science *265*, 676–679.
2. Antony, J.W., and Paller, K.A. (2017). Hippocampal contributions to declarative memory consolidation during sleep. In The Hippocampus from Cells to Systems, D.E. Hannula, and M.C. Duff, eds. (Springer International Publishing), pp. 245–280.
3. Marshall, L., Helgadóttir, H., Mölle, M., and Born, J. (2006). Boosting slow oscillations during sleep potentiates memory. Nature *444*, 610–613.
4. Ngo, H.V., Martinetz, T., Born, J., and Mölle, M. (2013). Auditory closed-loop stimulation of the sleep slow oscillation enhances memory. Neuron *78*, 545–553.
5. Kudrimoti, H.S., Barnes, C.A., and McNaughton, B.L. (1999). Reactivation of hippocampal cell assemblies: effects of behavioral state, experience, and EEG dynamics. J. Neurosci. *19*, 4090–4101.
6. Khodagholy, D., Gelinas, J.N., and Buzsáki, G. (2017). Learning-enhanced coupling between ripple oscillations in association cortices and hippocampus. Science *358*, 369–372.
7. Siapas, A.G., and Wilson, M.A. (1998). Coordinated interactions between hippocampal ripples and cortical spindles during slow-wave sleep. Neuron *21*, 1123–1128.
8. Maingret, N., Girardeau, G., Todorova, R., Goutierre, M., and Zugaro, M. (2016). Hippocampo-cortical coupling mediates memory consolidation during sleep. Nat. Neurosci. *19*, 959–964.
9. Staresina, B.P., Bergmann, T.O., Bonnefond, M., van der Meij, R., Jensen, O., Deuker, L., Elger, C.E., Axmacher, N., and Fell, J. (2015). Hierarchical nesting of slow oscillations, spindles and ripples in the human hippocampus during sleep. Nat. Neurosci. *18*, 1679–1686.
10. Xia, F., Richards, B.A., Tran, M.M., Josselyn, S.A., Takehara-Nishiuchi, K., and Frankland, P.W. (2017). Parvalbumin-positive interneurons mediate neocortical-hippocampal interactions that are necessary for memory consolidation. eLife *6*, e27868.
11. Gais, S., Mölle, M., Helms, K., and Born, J. (2002). Learning-dependent increases in sleep spindle density. J. Neurosci. *22*, 6830–6834.
12. Eschenko, O., Mölle, M., Born, J., and Sara, S.J. (2006). Elevated sleep spindle density after learning or after retrieval in rats. J. Neurosci. *26*, 12914–12920.
13. Clemens, Z., Fabó, D., and Halász, P. (2005). Overnight verbal memory retention correlates with the number of sleep spindles. Neuroscience *132*, 529–535.
14. Johnson, L.A., Blakely, T., Hermes, D., Hakimian, S., Ramsey, N.F., and Ojemann, J.G. (2012). Sleep spindles are locally modulated by training on a brain-computer interface. Proc. Natl. Acad. Sci. USA *109*, 18583–18588.
15. Mednick, S.C., McDevitt, E.A., Walsh, J.K., Wamsley, E., Paulus, M., Kanady, J.C., and Drummond, S.P. (2013). The critical role of sleep spindles in hippocampal-dependent memory: a pharmacology study. J. Neurosci. *33*, 4494–4504.
16. Kaestner, E.J., Wixted, J.T., and Mednick, S.C. (2013). Pharmacologically increasing sleep spindles enhances recognition for negative and high-arousal memories. J. Cogn. Neurosci. *25*, 1597–1610.
17. Niknazar, M., Krishnan, G.P., Bazhenov, M., and Mednick, S.C. (2015). Coupling of thalamocortical sleep oscillations are important for memory consolidation in humans. PLoS ONE *10*, e0144720.
18. Kurdziel, L., Duclos, K., and Spencer, R.M.C. (2013). Sleep spindles in midday naps enhance learning in preschool children. Proc. Natl. Acad. Sci. USA *110*, 17267–17272.
19. van der Helm, E., Gujar, N., Nishida, M., and Walker, M.P. (2011). Sleep-dependent facilitation of episodic memory details. PLoS ONE *6*, e27421.
20. Saletin, J.M., Goldstein, A.N., and Walker, M.P. (2011). The role of sleep in directed forgetting and remembering of human memories. Cereb. Cortex *21*, 2534–2541.
21. Wilhelm, I., Diekelmann, S., Molzow, I., Ayoub, A., Mölle, M., and Born, J. (2011). Sleep selectively enhances memory expected to be of future relevance. J. Neurosci. *31*, 1563–1569.
22. Oudiette, D., and Paller, K.A. (2013). Upgrading the sleeping brain with targeted memory reactivation. Trends Cogn. Sci. *17*, 142–149.
23. Farthouat, J., Gilson, M., and Peigneux, P. (2017). New evidence for the necessity of a silent plastic period during sleep for a memory benefit of targeted memory reactivation. Sleep Spindles & Cortical Up States *1*, 14–26.
24. Groch, S., Schreiner, T., Rasch, B., Huber, R., and Wilhelm, I. (2017). Prior knowledge is essential for the beneficial effect of targeted memory reactivation during sleep. Sci. Rep. *7*, 39763.
25. Lehmann, M., Schreiner, T., Seifritz, E., and Rasch, B. (2016). Emotional arousal modulates oscillatory correlates of targeted memory reactivation during NREM, but not REM sleep. Sci. Rep. *6*, 39229.
26. Schreiner, T., Lehmann, M., and Rasch, B. (2015). Auditory feedback blocks memory benefits of cueing during sleep. Nat. Commun. *6*, 8729.
27. Bal, T., and McCormick, D.A. (1996). What stops synchronized thalamocortical oscillations? Neuron *17*, 297–308.
28. Lüthi, A., and McCormick, D.A. (1998). Periodicity of thalamic synchronized oscillations: the role of Ca^{2+}-mediated upregulation of I_h. Neuron *20*, 553–563.
29. Contreras, D., Destexhe, A., Sejnowski, T.J., and Steriade, M. (1997). Spatiotemporal patterns of spindle oscillations in cortex and thalamus. J. Neurosci. *17*, 1179–1196.
30. Koupparis, A.M., Kokkinos, V., and Kostopoulos, G.K. (2013). Spindle power is not affected after spontaneous K-complexes during human NREM sleep. PLoS ONE *8*, e54343.
31. Rudoy, J.D., Voss, J.L., Westerberg, C.E., and Paller, K.A. (2009). Strengthening individual memories by reactivating them during sleep. Science *326*, 1079.
32. Oudiette, D., Antony, J.W., Creery, J.D., and Paller, K.A. (2013). The role of memory reactivation during wakefulness and sleep in determining which memories endure. J. Neurosci. *33*, 6672–6678.
33. Rasch, B., Büchel, C., Gais, S., and Born, J. (2007). Odor cues during slow-wave sleep prompt declarative memory consolidation. Science *315*, 1426–1429.
34. Sato, Y., Fukuoka, Y., Minamitani, H., and Honda, K. (2007). Sensory stimulation triggers spindles during sleep stage 2. Sleep *30*, 511–518.
35. Antony, J.W., and Paller, K.A. (2017). Using oscillating sounds to manipulate sleep spindles. Sleep (Basel) *40*, 1–8.
36. Lecci, S., Fernandez, L.M.J., Weber, F.D., Cardis, R., Chatton, J.-Y., Born, J., and Lüthi, A. (2017). Coordinated infraslow neural and cardiac oscillations mark fragility and offline periods in mammalian sleep. Sci. Adv. *3*, e1602026.

37. Ngo, H.V., Miedema, A., Faude, I., Martinetz, T., Mölle, M., and Born, J. (2015). Driving sleep slow oscillations by auditory closed-loop stimulation—a self-limiting process. J. Neurosci. *35*, 6630–6638.
38. Bastien, C., and Campbell, K. (1994). Effects of rate of tone-pip stimulation on the evoked K-complex. J. Sleep Res. *3*, 65–72.
39. Schellenberger Costa, M., Weigenand, A., Ngo, H.-V.V., Marshall, L., Born, J., Martinetz, T., and Claussen, J.C. (2016). A thalamocortical neural mass model of the EEG during NREM sleep and its response to auditory stimulation. PLoS Comput. Biol. *12*, e1005022.
40. Dehghani, N., Cash, S.S., Rossetti, A.O., Chen, C.C., and Halgren, E. (2010). Magnetoencephalography demonstrates multiple asynchronous generators during human sleep spindles. J. Neurophysiol. *104*, 179–188.
41. Andrillon, T., Nir, Y., Staba, R.J., Ferrarelli, F., Cirelli, C., Tononi, G., and Fried, I. (2011). Sleep spindles in humans: insights from intracranial EEG and unit recordings. J. Neurosci. *31*, 17821–17834.
42. Nir, Y., Staba, R.J., Andrillon, T., Vyazovskiy, V.V., Cirelli, C., Fried, I., and Tononi, G. (2011). Regional slow waves and spindles in human sleep. Neuron *70*, 153–169.
43. Oudiette, D., Santostasi, G., and Paller, K.A. (2013). Reinforcing rhythms in the sleeping brain with a computerized metronome. Neuron *78*, 413–415.
44. Batterink, L.J., Creery, J.D., and Paller, K.A. (2016). Phase of spontaneous slow oscillations during sleep influences memory-related processing of auditory cues. J. Neurosci. *36*, 1401–1409.
45. Göldi, M., van Poppel, E., Rasch, B., and Schreiner, T. (2017). Cueing memory during sleep is optimal during slow-oscillatory up-states. bioRxiv. https://doi.org/10.1101/185264.
46. Latchoumane, C.V., Ngo, H.-V.V., Born, J., and Shin, H.-S. (2017). Thalamic spindles promote memory formation during sleep through triple phase-locking of cortical, thalamic, and hippocampal rhythms. Neuron *95*, 424–435.e6.
47. Yamadori, A. (1971). Role of the spindles in the onset of sleep. Kobe J. Med. Sci. *17*, 97–111.
48. Steriade, M., McCormick, D.A., and Sejnowski, T.J. (1993). Thalamocortical oscillations in the sleeping and aroused brain. Science *262*, 679–685.
49. Cote, K.A., Epps, T.M., and Campbell, K.B. (2000). The role of the spindle in human information processing of high-intensity stimuli during sleep. J. Sleep Res. *9*, 19–26.
50. Dang-Vu, T.T., McKinney, S.M., Buxton, O.M., Solet, J.M., and Ellenbogen, J.M. (2010). Spontaneous brain rhythms predict sleep stability in the face of noise. Curr. Biol. *20*, R626–R627.
51. Schabus, M., Dang-Vu, T.T., Heib, D.P., Boly, M., Desseilles, M., Vandewalle, G., Schmidt, C., Albouy, G., Darsaud, A., Gais, S., et al. (2012). The fate of incoming stimuli during NREM sleep is determined by spindles and the phase of the slow oscillation. Front. Neurol. *3*, 40.
52. Renard, Y., Lotte, F., Gibert, G., Congedo, M., Maby, E., Delannoy, V., Bertrand, O., and Lecuyer, A. (2010). OpenViBE: an open-source software platform to design, test and use brain-computer interfaces in real and virtual environments. Presence Teleop. Virt. Environ. *19*, 35–53.
53. Delorme, A., and Makeig, S. (2004). EEGLAB: an open source toolbox for analysis of single-trial EEG dynamics including independent component analysis. J. Neurosci. Methods *134*, 9–21.
54. Rechtschaffen, A., and Kales, A. (1968). A Manual of Standardized Terminology, Techniques and Scoring System of Sleep Stages in Human Subjects (Public Health Service, U.S. Government Printing Office).
55. Mölle, M., Bergmann, T.O., Marshall, L., and Born, J. (2011). Fast and slow spindles during the sleep slow oscillation: disparate coalescence and engagement in memory processing. Sleep (Basel) *34*, 1411–1421.
56. Antony, J.W., Gobel, E.W., O'Hare, J.K., Reber, P.J., and Paller, K.A. (2012). Cued memory reactivation during sleep influences skill learning. Nat. Neurosci. *15*, 1114–1116.
57. Antony, J.W., Cheng, L., Pacheco, P., Paller, K.A., and Norman, K.A. (2017). Competitive learning modulates memory consolidation during sleep. bioRxiv. https://doi.org/10.1101/196964.

STAR★METHODS

KEY RESOURCES TABLE

REAGENT or RESOURCE	SOURCE	IDENTIFIER
Software and Algorithms		
MATLAB 2017A	MathWorks	https://www.mathworks.com
EEGLAB 13.4.4b	Delorme and Makeig, 2004 [47]	https://sccn.ucsd.edu/eeglab/index.php
OpenViBE	Renard et al., 2010 [48]	http://openvibe.inria.fr/
RStudio 1.0.153	R Core Team, 2015 [50]	https://www.r-project.org

CONTACT FOR REAGENT AND RESOURCE SHARING

Further information and requests for resources and reagents should be directed to and will be fulfilled by the Lead Contact, James Antony (jantony@princeton.edu).

EXPERIMENTAL MODEL AND SUBJECT DETAILS

Subjects

Subjects were asked to wake an hour earlier than normal in order to increase the chances of their napping successfully. They were also asked to refrain from drinking alcohol the night before and caffeine the morning of the experiment. Informed consent was obtained before and monetary reimbursement given after the study. Twenty-one (M = 21.8 years, range: 18-33, 10 female) and twenty-five volunteers (M = 22 years, range: 19 - 33, 15 female) from the Northwestern University community participated in experiments 1 and 2, respectively. Twenty-six volunteers (M = 21.2 years, range: 18-33, 10 female) from the Princeton University community participated in experiment 3. In experiments 1 and 2, subjects' data were included in the final dataset if they experienced one full round of cues during sleep and excluded otherwise. In experiment 3, the rate of cue presentation was slower because we waited to detect spindles before cuing; this, in turn, made it less likely that we would be able to get through a full round of cues. Therefore, we loosened our inclusion criterion *a priori* for experiment 3: Subjects were included if they experienced at least 50% of the overall cues (see Preregistered methods at https://osf.io/brndg/). Only two subjects received fewer than one full round of cues. In these cases, only the cued items from each group were analyzed. Data were excluded from subjects who did not receive the minimum number of cues (three, nine, and six subjects in experiments 1, 2, and 3, respectively). Written informed consent was obtained in a manner approved by the Princeton and Northwestern University Institutional Review Boards.

METHOD DETAILS

Stimuli

Subjects learned to associate 24 celebrities and 24 landmarks with 48 randomly-assigned environmental sounds bearing no relation to the pictures (e.g., a cat's meow, violin musical tones). The sounds lasted 0.5 s or less and were selected from a larger set used in another TMR study [32], so as to maximize the distinctiveness of the selected cues from each other.

In experiment 2, the oscillating sounds were created by modulating the amplitude of a white noise signal for 2 s, which was a mixture of sound frequencies from 20-1000 Hz with random amplitudes constant across the power spectrum [35]. The modulated sound alternated between 100% and 20% of the original amplitude in the form of a sine wave using the Tremolo function in Audacity software. Thus, the modulation did not change the maximum amplitude of the signal.

Design

The three experiments included sound-item association over-learning, item-location learning, pre-nap location testing, napping for 90 min, and post-nap item-location and sound-item testing. There was an additional phase before learning in which subjects viewed a different group of celebrities, landmarks, common objects, scrambled faces, and scrambled places, included to allow for training a wake EEG classifier. Those classification analyses are not described further in this article. The procedural details for each phase were as follows. During sound-item over-learning, subjects learned pairwise associations between 48 unique sounds and 48 new faces or places to a high degree of accuracy. During item-location learning, subjects learned the location of each picture against a background grid accompanied by its previously-associated sound. For the pre-nap test, subjects were tested on each picture location once, receiving feedback on the correct location after their guess. Then, subjects took a 90-min nap, during which learned sounds were randomly and repeatedly played to the subjects upon their entering SWS. Subjects returned to the lab 150 min after the nap to take tests on all item-location and sound-item associations.

Procedure

Pre-training

We fitted subjects with a 64-channel cap of electrodes along with two EEG mastoid electrodes and one EMG electrode on the chin. Two EOG channels were used for monitoring horizontal and vertical eye movements.

Sound-item overlearning

Subjects encoded sound-item pairs using repeated study-test cycles. During encoding, subjects viewed each picture for 4 s; concurrent with picture onset, a unique sound was played for 0.5 s. Sound-item mappings were random and different for each subject. A label indicating the correct name and spelling of the picture was shown below 2 s after picture onset, along with a re-presentation of the sound. During testing, subjects heard each sound alone and were asked to type in the corresponding picture label. Typing was only allowed to begin 1 s after sound offset. After submitting a response, subjects received feedback on whether their response was correct, along with a 4 s presentation of the picture and label, with the sound presented twice at 0 and 2 s. After the subject correctly produced a label twice in a row, the corresponding pair was dropped from further testing. Testing continued until all labels were correctly produced twice in a row. The pace of encoding and testing were thus at the subject's discretion in this phase.

Item-location learning

Next, subjects learned the location of each item against a background grid. Each picture was assigned to a random location −300 to 300 pixels from the center of the screen in horizontal and vertical directions. During encoding, subjects viewed the location of each picture for 3 s, accompanied by a single presentation of the picture's accompanying sound. Following encoding, we asked subjects to drag each picture from the center of the screen to where they remembered seeing it. After subjects made their location response, they viewed feedback of each picture in its correct location and heard its corresponding sound. When the recalled location was within 150 pixels of the correct location, the item dropped out from further testing. Subjects performed the task until they placed each pair within 150 pixels once.

Pre-nap item-location test

Following a 5-min break, subjects made their location response for each item once, followed by feedback. Items were again accompanied by their corresponding sound at presentation and feedback.

Nap

Subjects then took a nap in the laboratory against a background white-noise level of approximately 40 dB. All naps began in the afternoon between 12:30 and 14:30. Following online indications of SWS, 0.5 s sound cues were administered once every 4.5 s in a randomized order. In experiment 1, half of the cues were presented over multiple rounds (M = 7.24, range = 2.9-9.25). In experiment 2, all sounds were presented (M = 6.53, range = 2.62-10.77), with half of the sounds followed by 2 s of 15-Hz oscillating white noise. In experiment 3, all sounds were presented (M = 1.96, range = 0.56-4.0), with half 0.25 s after the end of a spindle and half 2.5 s after the end of a spindle. In all experiments, items in each group were equally split between celebrity and landmark categories. No individual cue caused an amplitude jump greater than 4 dB. Cues were immediately stopped upon online indications of arousal. If a subject had not heard a sufficient number of cues after 60 min, we cued during stage-2 NREM sleep (see above section: Subjects).

Post-nap item-location and sound-item tests

After the nap, subjects left the lab for 150 min. When they returned to the lab, they were tested on each item-location and then each sound-item pair without feedback. Sounds were omitted from the post-nap item-location test to prevent them from influencing memory for the later post-nap sound-item pair test. At the completion of the experiment, subjects were debriefed about the aims of the experiment.

EEG recording and pre-processing

Continuous EEG was recorded during the nap using Ag/AgCl active electrodes (Biosemi ActiveTwo, Amsterdam) using the same electrode layout and recording hardware at Northwestern (experiments 1 and 2) and Princeton (experiment 3). In experiment 3, for the purposes of real-time analyses, EEG data were collected using OpenViBE [52] rather than Biosemi software. Recordings were made at 512 Hz from 64 scalp EEG electrode locations. In addition, a vertical electrooculogram (EOG) electrode was placed next to the right eye, a horizontal EOG electrode was placed under the left eye, and an electromyogram (EMG) electrode was placed on the chin.

EEG data were processed using a combination of internal functions in EEGLAB [53] and custom-written scripts. Data were re-referenced offline to the average signal of the left and right mastoid channels and were down-sampled to 256 Hz. They were high-pass filtered at 0.1 Hz and low-pass filtered at 60 Hz in successive steps. Problematic channels were interpolated using the spherical method.

Sleep physiological analyses

Sleep stages were determined by an expert scorer according to standard criteria [54]. Table S1 shows the breakdown of stages for each condition as well as the number of cues occurring within each stage for all experiments. Note that sleep-staging rules require assigning stages based on whichever stage is more prevalent within the 30 s epoch, which can result in sounds occurring in stages that were not the intended targets. Artifacts (large movements, blinks, arousals, and rare, large deflections in single channels) during sleep were marked separately in 5 s chunks following sleep staging.

Spindles and SOs were calculated using established algorithms. Each of these scripts ignored 5 s intervals marked for rejection, effectively stitching together non-artifactual segments from all NREM epochs into a long, continuous EEG signal for further processing.

For spindles, sleep EEG data were bandpass-filtered between 11-16 Hz using a two-way, least-squares finite-impulse-response filter. Next, we calculated a root-mean-square (RMS) value for every time point using a moving window of ± 0.2 s for each channel separately. A threshold was determined by multiplying the standard deviation of the entire channel's signal by 1.5 [55]. Any RMS signal that crossed this threshold consecutively for 0.5- to 3 s was considered a spindle. Times for the start, negative peak (largest negative voltage value), and end of each spindle were recorded for alignment with sleep cues. We used this same RMS calculation for online spindle detection and offline cue-locked analyses.

For counting SOs, sleep EEG data were first low-pass filtered at 3.5 Hz. Any series of data points with successive positive-to-negative crossings lasting 0.75 to 2 s (corresponding to 0.5-1.3 Hz), a negative peak of −40 μV, and peak-to-peak amplitude of 75 μV was considered a slow oscillation. Similar to spindles, the start, negative peak, and end were recorded for later alignment with sleep cues.

Real-time spindle algorithm

In order to time cues relative to spindle events, we created an online spindle detection algorithm using open-source brain computer interface software called OpenViBE (http://openvibe.inria.fr/). OpenViBE allows for real-time processing of EEG data through MATLAB scripting and the translation of established offline detection scripts to an online format. Our offline algorithm used a band-pass (11-16 Hz) filter of the CPz voltage signal, RMS values based on a ± 0.2 s moving window, and a single-threshold constant value to detect spindles based on the standard deviation of the RMS signal over the whole recording.

However, in real-time, one cannot use the whole recording to calculate baseline thresholds or reliably reject artifacts. Therefore, we used a different algorithm for our online scripts (Figure S3). We relied on two band-pass filters and two spindle thresholds, instead of one for each. For filters, we chose the sigma band (11-16 Hz) and an equal-sized lower beta band that should have no spindle information (16-21 Hz). Generally, spindles only occur in the sigma band, but artifacts show up in both bands. As such, monitoring lower beta allowed us to detect (and discount) periods of time when broader signal artifacts were present. This algorithm was chosen based on its performance in detecting spindles on an online sleep spindles database (http://www.tcts.fpms.ac.be/~devuyst/Databases/DatabaseSpindles/).

The lower and upper thresholds were 2 and 4.5 times the RMS mean of the last 600 s of the recording for the baseline (lower beta) frequency bandwidth. If the RMS values in the spindle frequency bandwidth crossed the lower threshold, it was a candidate for a spindle. The length of time the RMS signal was above this lower threshold constituted its duration. To be categorized as a spindle, the duration was required to be 0.5-3 s and the RMS value was required to surpass the upper threshold at least once. Thus, if the spindle RMS values crossed the first minimum threshold without reaching the second maximum threshold, then it would not be categorized as a spindle, no matter its duration. Similarly, if it crossed the maximum threshold but did not have a duration between 0.5-3.0 s, it would also not be categorized as a spindle.

In order to present sounds, three conditions needed to be met: (1) spindle detection (2), RMS values were currently below the spindle threshold (so there was no candidate spindle presently ongoing) and (3) > 4.5 s elapsed since the onset of the previous sound. Once these conditions were met, sound information was sent to the presentation computer via UDP packets at different times depending on sound type. Early intervals of 0.25 s were chosen (as opposed to no delay) in order to avoid a scenario in which RMS values, while below the spindle threshold, still remained above baseline RMS values, thus causing a possible confound of sigma power at the $t = 0$. Late intervals of 3.5 s were chosen to be late enough to fall outside of the refractory period (see Figure 3). If a spindle occurred during this interval, the timer was reset and the next late sound could only occur 3.5 s after the onset of that (intervening) spindle. Note that the early and late intervals were calculated in a slightly different fashion: early cues were delivered 0.25 s after the offset of the preceding spindle, whereas late cues were delivered 3.5 s after the onset of the preceding spindle (~2.5 s after the offset).

Spontaneous (non-TMR) sleep data

Data collected during similar experiments from other subjects (N = 28, age range: 18-30) were used to validate the dynamics of the spindle refractory period in the absence of TMR cues. The no-sounds control condition in a published study [56] was used for 16 subjects. In all cases, subjects performed pre-learning memory tasks. These data were acquired using Neuroscan software at a sampling rate of 1000 Hz with a bandpass of 0.1–100 Hz. Tin electrodes in an elastic cap were placed at 21 standard scalp locations, left and right mastoids, lateral to the right eye, under the left eye, and on the chin. Data were downsampled to 250 Hz, re-referenced to average mastoids, and filtered between 0.4-60 Hz in successive steps using a 2-way least-squares finite impulse response filter. Because we used an electrode montage that did not include CPz, we used Pz instead. Analyses paralleling Figures 3A, 3B, and 3D are reproduced using this dataset in Figure S2.

QUANTIFICATION AND STATISTICAL ANALYSIS

All statistical analyses in all experiments used every subject (Experiment 1: N = 18; Experiment 2: N = 16; Experiment 3: N = 20). These sample sizes were determined based on previous studies [31, 32] and the sample size in Experiment 3 was pre-registered (https://osf.io/brndg/). All error measurements indicate standard error of the mean (SEM).

Behavioral dependent variables and analyses

We used an adjusted forgetting score as our primary dependent variable. Forgetting, calculated as post-nap error minus pre-nap error, significantly correlates with pre-nap error. Items with highly accurate pre-nap recall face ceiling effects (e.g., an error of

only 2 pixels cannot be improved across the nap by more than 2 pixels) and those with poor pre-nap accuracy show a regression to the mean (e.g., an incorrectly recalled location, when very distant from the correct location, is likely to be recalled more accurately after the nap, even by chance). Therefore, we calculated the linear relationship between pre-nap score and forgetting (post-nap – pre-nap score) pooled across subjects in the present data (Figure S1). Then we subtracted each forgetting score from the forgetting expected from this linear relationship (i.e., the residual) and, because the residual analysis zeros out forgetting, we added back the mean raw forgetting value to produce the adjusted forgetting score used for all reported analyses.

We assessed behavioral cueing effects between conditions using within-subject t tests on mean error for each subject and condition. This analysis is repeated for Figures 1B, 1F, and 4C.

Physiological analyses

As fast spindles tend to correlate with subsequent memory [2], we chose a cluster of centroparietal electrodes (Cz, Cp1, Cpz, Cp2, Pz) for physiological analyses *a priori* as in a previous study [57], as they are the scalp locations where fast spindle power is maximum [41]. We did not investigate other clusters, although it can be seen in the topographical maps in Figure 2B that this cluster includes the scalp regions associated with memory performance in the spatial recall test. Cue-locked spindle density measures (e.g., 0-2 s, 2-4 s) indicate the number of spindles per minute that started in a particular interval (i.e., divided by the length of the interval). In Figures 1D, 1E, and 1G, we assessed differences in spindle density at different time segments or across different conditions using within-subject t tests. In Figure 2A, we assessed post-cue spindle density differences based on pre-cue status using a repeated-measures ANOVA with two factors, pre-cue spindle status (present versus not) and post-cue interval (0-2 versus 2-4 s). In spindle analyses combining data from experiments 1 and 2, we collapsed the cued-oscillation and cued-only conditions, due to the nonsignificant effect of the oscillation on spindle measures.

We chose electrode CPz where single channels were more appropriate, such as graphing RMS over time in Figures 2B and 4F. We corrected for multiple comparisons in two steps. First, we randomly permuted better-remembered and worse-remembered conditions 400 separate times. After each permutation, we calculated the maximum number of consecutive time values that differed from $p < 0.05$, yielding a null distribution of maximum-consecutive-time points. We then compared the number of consecutive significant time points to the null distribution, yielding a family-wise error value. Any true time segment exceeding the 95th percentile of the null distribution (indicating a family-wise p value < 0.05) was deemed significant.

Spindle refractory period analyses

Analyses in Figure 3 were performed on data from electrode CPz. Inter-spindle lags were found by calculating the amount of time between successive spindles. Relative RMS power was calculated by performing fast Fourier transforms on artifact-free NREM periods, sorting data into 200 frequency bins between 0-1 Hz, and calculating within-subject relative power. To calculate RMS autocorrelations, we first obtained all RMS values between −10 to +10 s surrounding each spindle peak for each subject, mean-normed for the average RMS values from a wider −30 to +30 s block. Next, we calculated correlations between every time lag and $t = 0$ separately across spindle trials. Finally, we plotted these mean correlations with standard errors with arrows where correlations were both at a local maxima or minima and significantly different from zero using within-subject t tests. Bivariate spindle and sound lag analyses were calculated by taking each moment in the recording and binning it into 0.5 s segments by the amount of time since the onset of the most recent sound and the onset of the most recent spindle. Moments when spindles started were marked to later calculate the likelihood of a spindle occurring in that given bivariate bin. Finally, two-dimensional color plots were produced for sound intervals of 0 – 4.5 s (9 bins) and spindle lags of 0 – 10 s (20 bins), and horizontal and vertical bar graphs indicated the means across each dimension.

Experiment 3 physiological analyses

In Figure 4B, we assessed the efficacy of the real-time algorithm using a within-subject t test on the percentage of times the offline spindle had a pre-cue spindle starting between −2.5 and 0 s relative to the cue in each condition. In Figure 4D, we used a repeated-measures ANOVA to assess spindle density by post-cue interval (0-2 versus 2-4 s) and cue type (Early versus Late). In Figure 4E, we performed the same analysis, except using slow oscillation density rather than spindle density. We also investigated the specificity of the above two effects in a three-way repeated-measures ANOVA by assessing density event type (spindles versus SOs) and post-cue interval (0-2 versus 2-4 s) and cue type (Early versus Late). In Figure 4G, we assessed spindle inter-spindle lag differences between the experiments with an across-subject t test on the fraction of spindles beginning with very short lags less than 1.5 s (Experiment 1 & 2: N = 34; Experiment 3: N = 20).

Sound-item memory analyses

Sound-item memory contrasts were performed as within-subject t tests between cueing groups in all experiments.

DATA AND SOFTWARE AVAILABILITY

Based on the results of experiments 1 and 2, the hypotheses, methods, and planned analyses for experiment 3 were pre-registered at https://osf.io/brndg/. All code and results will be placed there upon publication.

Current Biology, Volume *28*

Supplemental Information

Sleep Spindle Refractoriness Segregates Periods of Memory Reactivation

James W. Antony, Luis Piloto, Margaret Wang, Paula Pacheco, Kenneth A. Norman, and Ken A. Paller

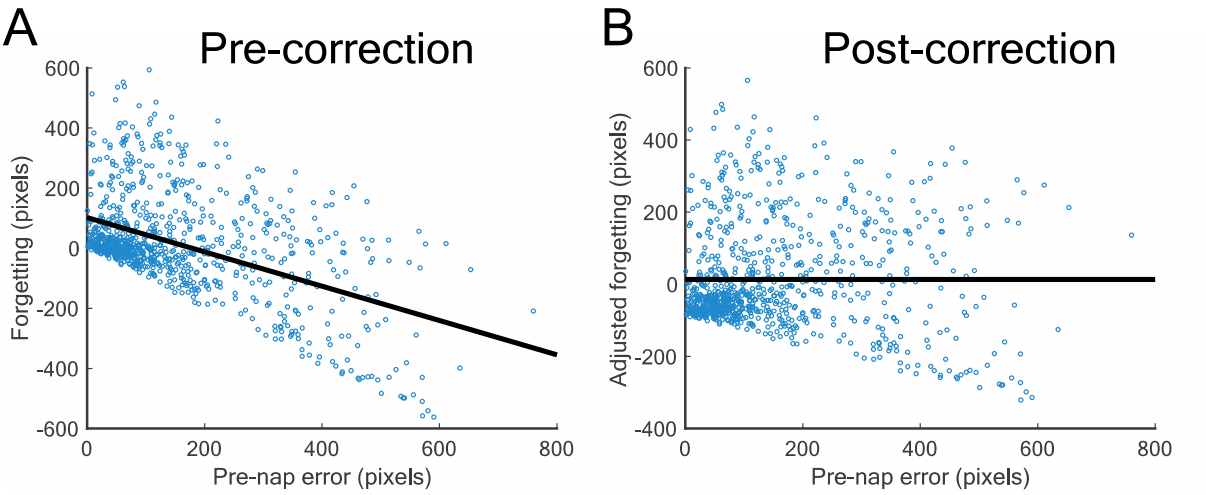

Figure S1. Residual analysis used in the forgetting metric. Related to Figure 1. (A) Pre-nap error significantly predicts forgetting (post- – pre-nap error). **(B)** Corrected (residual) forgetting values after regressing out pre-nap error.

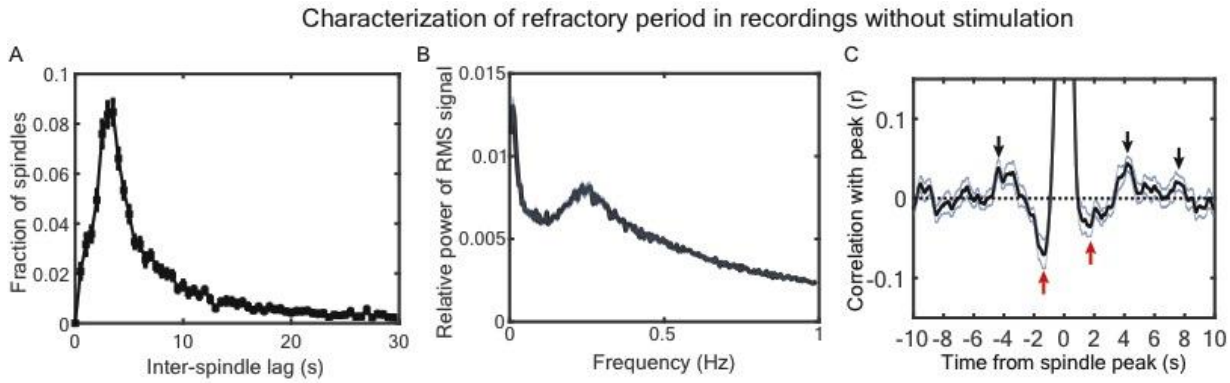

Figure S2. Spindle refractory period analyses on non-TMR data. Related to Figure 3. A-C represent a variant of the graphs from Figure 3A, B, and D using data from an experiment with no TMR cues (*N*=28). We relied on data from the Pz electrode because EEG acquisition did not include CPz. All error measurements indicate SEM.

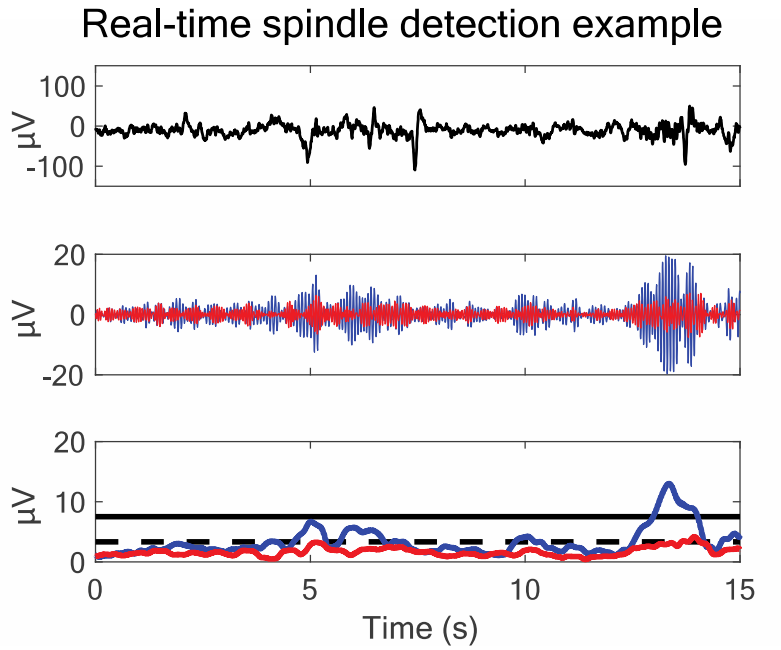

Figure S3. Example of a spindle detected by online spindle algorithm. Related to Figure 4. (Top) Raw EEG signal. **(Middle)** Signals filtered in the sigma (11-16 Hz, blue) and lower beta (16-21 Hz, red) bands. **(Bottom)** RMS sigma (blue) and lower beta (red) signals along with the first (dashed black) and second (solid black) spindle thresholds, which were multiplications of 2 and 4.5 times the mean lower beta power, respectively. Any sigma signal above the first threshold between 0.5 – 3 s and above the second threshold at any point was considered a spindle. One spindle was thus detected near the end of the interval.

Time in each stage (min)		Wake	S1	S2	S3	REM
Exp 1	Mean	27.69	5.78	24.25	20.81	3.08
	SEM	3.96	0.69	2.90	4.20	1.07
Exp 2	Mean	21.22	5.97	22.69	20.16	4.28
	SEM	3.51	0.95	2.54	3.23	1.35
Exp 3	Mean	21.43	5.83	26.68	17.45	4.98
	SEM	3.59	0.56	2.49	2.41	1.53
Mean sounds per stage						
Exp 1	Mean	4.17	2.61	43.11	120.50	0.00
	SEM	1.50	0.97	13.24	19.91	0.00
Exp 2	Mean	1.81	1.44	97.31	217.25	0.00
	SEM	0.70	0.83	26.90	30.97	0.00
Exp 3	Mean	1.30	0.80	35.90	54.30	0.85
	SEM	0.42	0.30	3.97	9.88	0.43

Table S1. Sleep staging and cue quantification. Related to Figures 1 & 4. Mean amount of time in each sleep stage (min ± SEM) is displayed together with the number of cues per stage for Experiments 1, 2, and 3.

Autocorrelation peaks

Peak time (s)	Peak type
-8.414	Negative
-7.277	Negative
-5.941	Positive
-4.727	Negative
-3.240	Positive †
-1.480	Negative
0.000	Positive
1.480	Negative
3.016	Positive
4.496	Negative
5.547	Positive
7.723	Positive
8.371	Negative

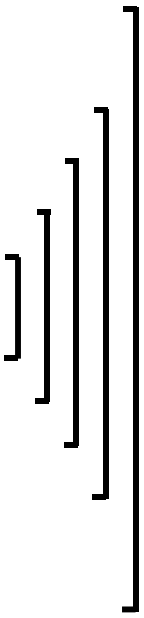

Table S2. Timing of autocorrelation peaks in sigma RMS signal. Related to Figure 3. Shown are all positive and negative autocorrelation peaks with each time point and $t = 0$ from Figure 3D. Brackets indicate approximately symmetric peaks around $t = 0$. All peaks are significant at $p < 0.05$ level, except †, where $0.05 < p < 0.1$.